

Sensing multiatom networks in cavities via photon-induced excitation resonance

Pritam Chattopadhyay,^{1,*} Avijit Misra,^{1,2,†} Saikat Sur,^{1,‡} David Petrosyan,^{3,§} and Gershon Kurizki^{1,¶}

¹*Department of Chemical and Biological Physics & AMOS,
Weizmann Institute of Science, Rehovot 7610001, Israel*

²*Department of Physics, Indian Institute of Technology (ISM), Dhanbad, Jharkhand 826004, India*

³*Institute of Electronic Structure and Laser, FORTH, GR-70013 Heraklion, Greece*

We explore the distribution in space and time of a single-photon excitation shared by a network of dipole-dipole interacting atoms that are also coupled to a common photonic field mode. Time-averaged distributions reveal partial trapping of the excitation near the initially excited atom. This trapping is associated with resonances of the excitation at crossing points of the photon-dressed energy eigenvalues of the network. The predicted *photon-induced many-atom trapped excitation* (PIMATE) is sensitive to atomic position disorder which broadens the excitation resonances and transforms them to avoided crossings. PIMATE is shown to allow highly effective and accurate sensing of *multi-atom* networks and their disorder.

Effects of many-atom coupling to either cavity or waveguide fields [1–4] are becoming increasingly accessible by experiments. Here we predict a hitherto unexplored effect of photon-induced many-atom trapped excitation (PIMATE). PIMATE consists of partial spatial trapping of a single excitation shared by a network of dipole-dipole interacting atoms that are simultaneously strongly coupled to a photonic field mode. This partial trapping is associated with resonances of the excitation at crossing points of the photon-dressed energy eigenvalues of the network. Such crossing points are shown to occur at specific values of resonant dipole-dipole interaction (RDDI) [5] for a given atomic coupling strength to the photonic mode.

PIMATE is shown to be highly sensitive to the *long-range* (retardation) characteristics of RDDI [6–9] and its *disorder* in the many-atom network. Unlike single-body Anderson localization (AL) [10–14] or many-body localization (MBL) [15–17], disorder in the many-atom system *weakens* PIMATE by broadening the excitation resonances and transforming the crossings into pseudo-crossings. As shown, the many-atom disorder can be sensed by non-demolition monitoring of the time-dependent and time-averaged excitation of the initially-excited atom, owing to the properties of PIMATE.

The precision of such sensing is statistically quantified by the quantum Fisher information (QFI) [18–20]. We show that the *QFI of estimating the many-atom distribution diverges at the crossing-points*. This divergence yields highly enhanced precision of mapping out the many-atom distribution and its disorder merely by a *single measurement* of the excitation of a *single (initially-excited) atom*. In contrast, without the photon-induced trapping that underlies PIMATE, we would need to probe many atoms in RDDI-coupled disordered atom chains in open space and perform many more measurements of each atom in order to obtain similar information. Thus, PIMATE constitutes a novel, highly effective *single-atom sensor* of *multi-atom* disorder [21].

MODEL

We consider N spatially distributed atoms coupled to a field mode in a waveguide or a cavity (Fig. 1(i),(ii)). As a possible experimental scenario, we may envisage N atoms with levels $|g\rangle$, $|e\rangle$, $|r\rangle$ placed in a microwave cavity that is near-resonant with the $|e\rangle \rightarrow |r\rangle$ transition between the Rydberg states $|e\rangle$ and $|r\rangle$ (Fig. 1b).

Let us assume that all the atoms $j = 1, \dots, N$ in the system are initially in their ground states $|g_j\rangle$, and a laser field is applied as an *abrupt quench* which, combined with a microwave field, may result in transition to a Rydberg states $|g_j\rangle \rightarrow |e_j\rangle, |r_j\rangle$. The *effective Hamiltonian* of this combined atom-cavity system *following the quench* is then ($\hbar = 1$)

$$H = \omega a_0^\dagger a_0 + \sum_{j=1}^N \omega_0 |r_j\rangle \langle r_j| + \sum_{i,j=1;i < j}^N M_{ij} (|e_i r_j\rangle \langle r_i e_j| + H.c.) + \sum_{j=1}^N (\kappa_j a_0 |r_j\rangle \langle e_j| + H.c.). \quad (1)$$

Here $|r_j\rangle$ and $|e_j\rangle$ constitute the upper and lower states, respectively, separated by the energy ω_0 ($\hbar = 1$) of the effective j -th two-level atom (TLA); M_{ij} is the resonant dipole-dipole interaction (RDDI) strength between the i and j TLAs, κ_j is the coupling strength of the j -th TLA with the near-resonant cavity mode at the frequency ω , characterized by annihilation operator a_0 . The atoms have transition frequency $\omega_0 = k_0 c$, so that their *near-zone* interaction separation $R_{ij} \ll k_0^{-1}$ corresponds to RDDI of the form $M_{ij} \sim (k_0 R_{ij})^{-3}$. By contrast, for R_{ij} beyond the near-field zone, RDDI must be described by its full separation-dependent real self-energy matrix [5, 22–25]

$$\begin{aligned} \text{Re}(M_{ij}) &= \gamma J_\Sigma(k_0 R_{ij}), \\ \text{Im}(M_{ij}) &= \gamma J_\Pi(k_0 R_{ij}), \end{aligned} \quad (2)$$

$$\begin{aligned} J_\Sigma(k_0 R_{ij}) &= -\frac{3}{2} \left[\frac{\cos(k_0 R_{ij})}{(k_0 R_{ij})^3} + \frac{\sin(k_0 R_{ij})}{(k_0 R_{ij})^2} \right], \\ J_\Pi(k_0 R_{ij}) &= \frac{3}{4} \left[\frac{\cos(k_0 R_{ij})}{(k_0 R_{ij})^3} + \frac{\sin(k_0 R_{ij})}{(k_0 R_{ij})^2} - \frac{\cos(k_0 R_{ij})}{(k_0 R_{ij})} \right]. \end{aligned}$$

* contributed equally; pritam.chattopadhyay@weizmann.ac.il

† contributed equally; avijitmisra@iitism.ac.in

‡ contributed equally; saikat.sur@weizmann.ac.il

§ dap@iesl.forth.gr

¶ gershon.kurizki@weizmann.ac.il

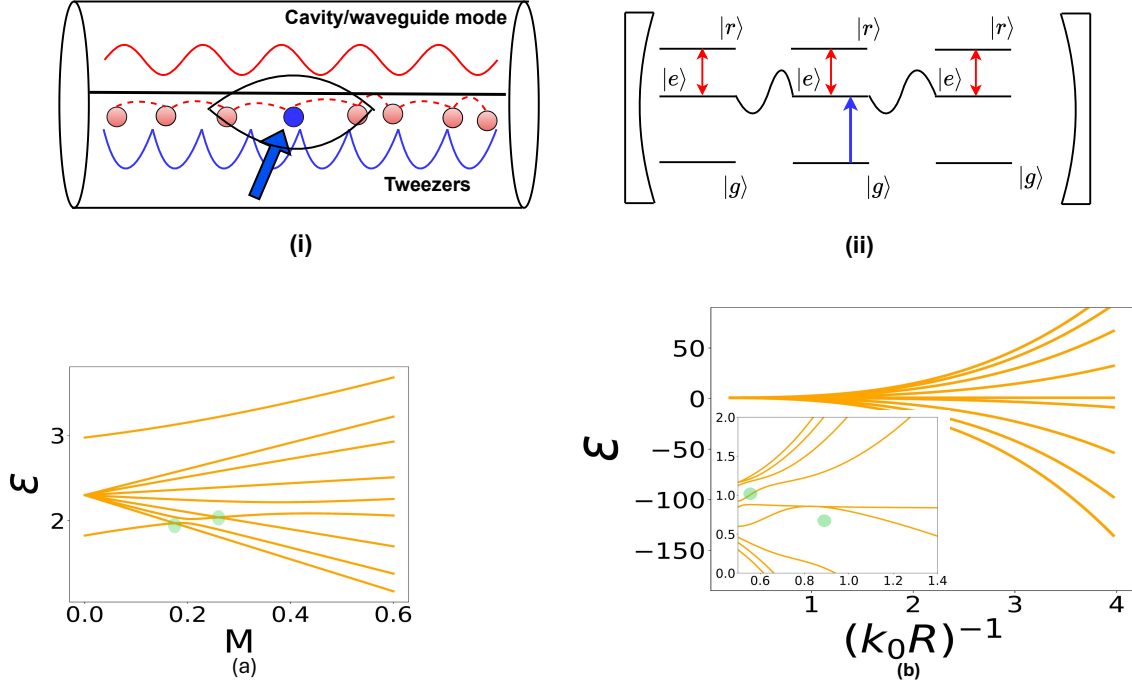


FIG. 1: Inset (i) Schematic of ordered or disordered dipole-dipole interacting N -atom network in a waveguide. The blue arrow denotes a laser beam focused on a chosen atom that excites it to a state where it can interact with the cavity mode. Inset (ii) Schematic of three-level N Rydberg atoms in a microwave cavity, where a chosen atom (here in the middle) is excited from $|g\rangle$ to $|e\rangle$ by a focused laser beam, from which it can be further excited to the Rydberg state $|r\rangle$ by a microwave photon resonant with the cavity mode. Main figure: Single-excitation eigenvalues for an open chain of $N = 8$ atoms as a function of the RDDI M and fixed atom-cavity coupling κ_j , assuming negligible dissipation (suppressed by a cavity or a photonic bandgap). The system is described by Hamiltonian parameters: $\omega - \omega_0 = 0.2\gamma$, $\kappa_j = 0.2\gamma$ where ω is the cavity frequency and γ is the free-space single-atom radiative decay rate. (a) Nearest neighbor (NN) RDDI, (b) same for long-range non-nearest-neighbor (NNN) RDDI as a function of separation $k_0 R$ for negligible dissipation. The crossing points and the pseudo-crossing points of eigenvalues on all plots are marked by circles.

where γ is the single-atom radiative decay rate at ω_0 , and $\Sigma(\Pi)$ denotes the atomic dipole being parallel (perpendicular) to the multi-atom one-dimensional open chain.

In general, one should also account for the *dissipative*, radiative effect associated with the *imaginary* self-energy by matrix that complements the real self-energy matrix M_{ij} . The dissipation analysis is relegated to the SI. In the main text, we assume *negligible radiative dissipation* as in a high-Q cavity or in a photonic bandgap structure [15–17, 26].

We assume that only one atom is initially in state $|r\rangle$, the remaining atoms are in state $|e\rangle$, while the cavity is empty. The subsequent dynamics will then be restricted to the *one-excitation subspace*.

RESULTS

The most general time-dependent state of the combined field-atom system (1) in the *single-excitation sector* is,

$$|\psi(t)\rangle = \sum_{j=1}^N \alpha_j(t) |e, \dots, r_j, \dots, e, 0\rangle + \beta(t) |e \dots e, 1\rangle \quad (3)$$

Here 0 and 1 denote the photon number in the cavity mode. The time-dependent coefficients $\alpha_j(t)$ and $\beta(t)$ in Eq. (3) can be obtained from the Schrödinger equation $|\dot{\psi}(t)\rangle = -iH|\psi(t)\rangle$, which yields a set of coupled differential equations for $\alpha_j(t)$ and $\beta(t)$, that can, in turn, be cast to a set of coupled algebraic equations in the Laplace domain. The vector of Laplace-transformed excitation amplitudes has then the form,

$$\begin{aligned} s\hat{\beta}(s) &= -i\omega\hat{\beta}(s) - i \sum_j \kappa_j^* \hat{\alpha}_j(s) + \hat{\beta}(0), \\ s\hat{\alpha}_j(s) &= -i\omega_0\hat{\alpha}_j(s) - i\kappa_j\hat{\beta}(s) - i \sum_{j'} M_{jj'} \hat{\alpha}_{j'}(s) + \hat{\alpha}_j(0), \end{aligned} \quad (4)$$

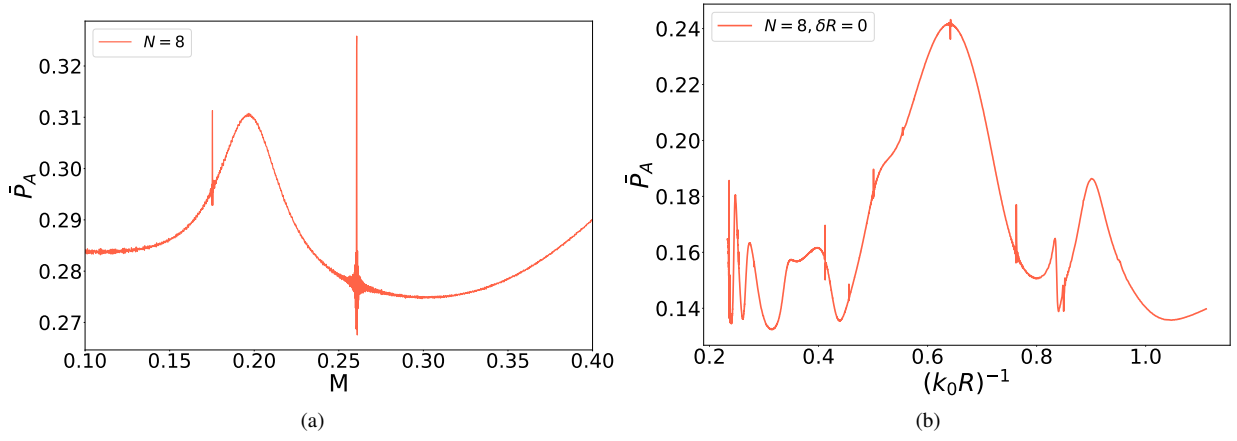


FIG. 2: (a) Resonances of the time-averaged excitation probability as a function of M (dipole-dipole interaction strength) assuming *negligible dissipation* for the nearest-neighbor (NN) interaction. Partial trapping occurs at the crossing point of the eigenvalue spectrum in perfectly periodic chains, (b) Same, as a function of $k_0 R$ for the *long-range* (NNN) interaction. The Hamiltonian parameters are as in Fig. 1: $\omega - \omega_0 = 0.2\gamma$, $\kappa_j = 0.2\gamma$, $T = 10000$ where T denotes the total time over which the average is computed.

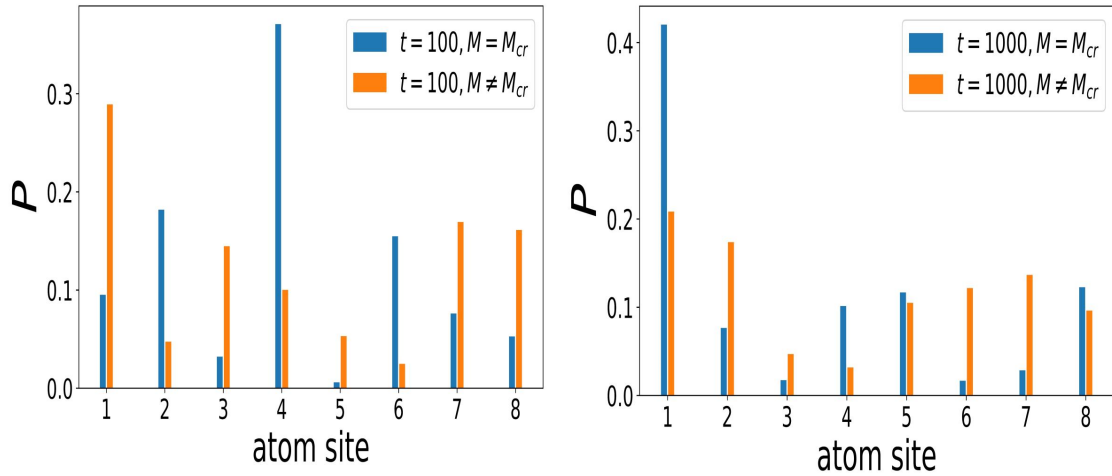


FIG. 3: Excitation probability of the atoms at different times in the NN case of Fig. 2a at the crossing/resonance point $M = M_{cr}$ (in blue) and at the non-resonance point $M \neq M_{cr}$ (in orange). The Hamiltonian parameters are as in Fig. 1, 2. Partial trapping of the excitation at the site of the initially excited atom (here atom 1) is seen to occur at long times (right panel) *only at the crossing point* in the NN case.

Substituting the solution for $\hat{\beta}(s)$, under the assumption that $\hat{\beta}(0) = 0$ (initially excited j th atom and empty cavity), we can write the following solution for the *vector* of many-atom excitation amplitudes, $\hat{\alpha}(s) \equiv (\hat{\alpha}_1(s), \hat{\alpha}_2(s), \dots, \hat{\alpha}_N(s))^T$:

$$\hat{\alpha}(s) = \mathbf{A}^{-1}(s)\hat{\alpha}(0) = |\mathbf{A}(s)|^{-1} \text{adj}(\mathbf{A}(s))\hat{\alpha}(0). \quad (5a)$$

where, under the assumption of *negligible dissipation* discussed above, the matrix elements have the form

$$\mathbf{A}_{jj'}(s) = (s + i\omega_0)\delta_{jj'} + \frac{\kappa_j \kappa_{j'}^*}{(s + i\omega)} + iM_{jj'}(1 - \delta_{jj'}). \quad (5b)$$

Imaginary roots of the polynomial obtained from $|\mathbf{A}(s)|$ by setting $s = \epsilon$ provide us with the actual spectrum of eigenvalues ϵ . If $\{\epsilon\}$ are the solutions to $|\mathbf{A}(\epsilon)| = 0$, then $\prod_m (s - \epsilon_m)^m = 0$; where the index m denotes the order of the pole ϵ_m . The solution to $\hat{\alpha}(s)$ can be then expressed as

$$\hat{\alpha}(s) = \frac{\text{adj}(\mathbf{A}(s))\hat{\alpha}(0)}{\prod_{m=1}^l (s - \epsilon_m)^m} = \sum_{m=1}^l \sum_{j=1}^m \frac{\mathbf{r}_{m,j}}{(s - \epsilon_m)^j}, \quad (6)$$

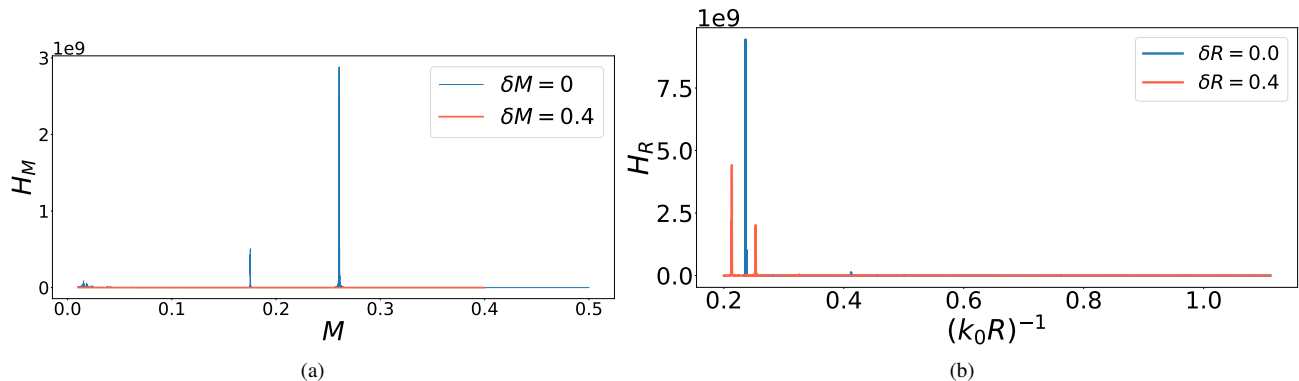


FIG. 4: (a) Variation of the quantum Fisher information without dissipation for *nearest-neighbor* (NN) interacting $N = 8$ atoms as a function of M (dipole-dipole interaction strength) in the presence of off-diagonal randomness (red solid line) and without randomness (blue solid line). (b) Same, for *long-range NNN interaction* for negligible dissipation as a function of $1/(k_0 R)$ in the presence of off-diagonal randomness (red solid line) and without randomness (blue solid line). The Hamiltonian parameters are as in Fig. 1, 2.

where $r_{m,j}$ is the residue corresponding to the pole ϵ_m of order j . The solution (6) has been obtained by the technique of partial fraction expansion of proper rational functions which can have different kinds of poles: Simple poles that are located far from critical points of the energy or higher-order poles located at critical points. The Laplace transform of the latter poles is divergent in the time domain. Any crossing of energy eigenstates corresponds to higher-order poles. This crossing in turn gives rise to exponential divergence in the residue, allowing the analytical evaluation of the dynamics (see SI).

In particular, the dependence of the time-averaged excitation probability of the initially excited atom \bar{P}_A on the averaging time T is exponential if there is no higher-order pole, $\bar{P}_A \propto e^{T(\lambda_m^* + \lambda_m)}$ where $\{\lambda_m\}$ are the roots of the polynomial expression in (6), and polynomial $\bar{P}_A \propto T^{2d-1}$ when there is a pole of order d .

Perfectly ordered chains: Setting $s = -i\epsilon$ in Eq. (6) yields the poles which correspond to crossing points as a function of M (Fig. 1a). In the nearest-neighbor (NN) regime, we find a *single* crossing point, regardless of the atom number ($N = 8$ is shown). By contrast, in the non-nearest neighbor (NNN) regime of long-range RDDI (Fig. 1b), there are multiple crossing points on account of the *non-monotonic dependence* of M on $k_0 R$. The corresponding time-averaged excitation probability of the initially excited atom has narrow resonances at inter-atomic separations R or equivalently at RDDI values M that correspond to those crossing points (Fig. 2a).

For long-ranged (NNN) RDDI, *local minima* (anti-localization dips) are observed at the pseudo-crossings and local maxima (localization) at the crossings of the time-averaged excitation probability (see Fig. 2b) only if the dissipative effects are suppressed, as for ω_0 inside a band gap. Otherwise, large dissipation predominantly (but not completely) delocalizes the excitation (see below).

Randomized chains: Let the position of the j th atom be X_j and its new position be $X_j + \delta X_j$ after introducing the disorder,

where δX_j is drawn from a Gaussian distribution around the mean X_m and standard deviation ΔX . We assume that ΔX is much less than $|X_j - X_{j+1}|$. These positional disorders result in a spread in the distribution of M_{ij} which is *non-Gaussian*, although derived from positions X_j having a Gaussian distribution.

The changes in PIMATE due to such randomness are illustrated in Fig. S1. The randomness transforms the crossing points in the eigenvalue spectrum into pseudo-crossing. Introducing randomness into the system causes eigenvalue repulsion, that is asymptotically associated with the sine kernel [27, 28]. This repulsion eliminates any degeneracy in the system's eigenspectrum. Thus a gap opens up at the crossing point when randomness is introduced in M (Fig. S1 a, b), transforming it into a pseudo-crossing point. The gap increases as randomness grows. In the NNN regime of long-range RDDI, with randomized couplings, no crossing is observed; only multiple avoided crossings arise. Consequently, there are no distinct peaks in the time-averaged excitation probability distribution (Fig. S1 c, d).

Dynamics: The dynamics of the system can be described by a collection of snapshots of the excitation probability for (of atoms in the chain) different time intervals at the crossover (resonance) point and non-resonance point and then time-averaged.

The high recurrent excitation probability of the initially excited atom at the resonance position (crossing point) compared to an atom at a non-resonant position (at a non-crossing point) at different time snapshots indicates partial trapping of the excitation at the crossover point (Fig. 3).

ESTIMATION OF NETWORK PARAMETERS

The excitation probability of the initially excited TLA, $|\alpha_j(t)|^2$ can be used to *estimate* M for the NN interaction and

R_{ij} for the *long-range NNN interaction* using the important tool of quantum Fisher information [20, 29–31]. The precision of estimating M or R_{ij} is restricted by the Cramér-Rao bound for the error variance which reads as [30] $\text{Var}(M) \geq \frac{1}{NH(M)}$, where $H(M)$ is the relevant quantum Fisher information (QFI) and N is the number of measurements. Here we measure the reduced time-averaged density matrix ρ_A of the atom A , which is diagonal in the computational basis, and hence the QFI for estimating M can be expressed as [20]

$$H_{M(R)} = \sum_{i=1}^2 \frac{|\frac{\partial \rho_A^i}{\partial M(R)}|^2}{\rho_A^i}, \quad (7)$$

where $\rho_A^1 = |\alpha_A(t)|^2$ and $\rho_A^2 = 1 - |\alpha_A(t)|^2$. As shown below, for a specific single-atom coupling strength κ , the QFI has a peak or divergence at a particular point on RDDI M , which implies *maximized precision of estimating M* . This is explained by the features of the Laplace transform solution of the α_j .

From the location of the divergence, one can also estimate the κ value. In the multi-atom case, the degeneracies of the eigenvalues for some particular values of M cause a divergence in the residue and thus in the time-averaged excitation probability (as shown in Fig. 2) for the NN and long-range interaction scenarios with and without randomness in the system. For this particular value of M , QFI has a peak (Fig. 4) which occurs at the crossing points in the eigenvalue spectrum. Therefore, by appropriately tuning the parameters of the system to the region where the QFI peak occurs, the efficiency and precision of the excitation measurement are maximized.

The washout of the excitation peak in Fig. S1c corresponds to the loss of QFI divergence in the nearest neighbor (NN) regime, which is a signature of randomness in the system. In the NNN long-range interaction regime, we observe diminished peaks of QFI in the presence of randomness (Fig. 4).

The variation of the peak of the logarithmic Fisher information with the randomness in M for the NN interaction and with R for the long-range NNN interaction is shown in the SI. With the increase in randomness, *the peak value of the Fisher information diminishes* (Fig. S6). This allows us to identify the presence of randomness in the network.

DISCUSSION

The ability explored here to sense and design interacting-atom arrays, by controlling the couplings of the atoms to a

cavity [1, 26] or waveguide [2, 6, 7, 23] and/or their resonant dipole-dipole interaction (RDDI) [8] is of interest since they constitute a platform for studies in quantum technologies and the fundamentals of light-matter interaction. Their collective behavior has been shown to yield a much richer diversity of phenomena compared to few atoms, with both fundamental and technological consequences. Precise control of interactions among atoms and their couplings to a cavity or waveguide fields is key to the success of such applications. For example, the fidelity of quantum gates in atomic quantum information processing and computation [32–36] depends on the interatom interactions. Hence, it is important to estimate the distribution of the RDDI and fine-tune it according to needs.

Towards these goals, we have revealed the hitherto unknown photon-induced many-atom trapped excitation (PIMATE) at the crossing of the field-dressed many-atom eigenvalues in the single-excitation domain. Retarded RDDI among atoms has been shown to drastically affect PIMATE beyond the near zone. It is important to distinguish PIMATE from *static excitation trapping* at a particular site. As shown in the SI, in PIMATE the excitation oscillates in time, and trapping is only evident following long-time averaging.

Positional disorder in the multi-atom chain array, which results in a spread in the RDDI; and the variability of the coupling strength of individual atoms to the field mode (SI) have been shown to be detrimental to PIMATE. Thus, *randomization can be detected by the absence of PIMATE*, which provides a new perspective for distinguishing a localized phase from the ergodic phase [16, 37, 38].

We have shown that PIMATE or its absence due to disorder can be monitored with enhanced precision or equivalently via very few (even one) measurements because the *quantum Fisher information (QFI) diverges at a crossing of the photon-dressed energy eigenvalues*. This finding is reminiscent of the role of *dynamical control* in enhancing the QFI and thereby the precision of quantum thermometry [39], as well as the ability of *criticality behavior* in quantum many-body systems to achieve enhanced-precision thermometry, magnetometry [40–42], or environment parameter estimation by a quantum probe [43–45].

-
- [1] Mauro Paternostro, GS Agarwal, and MS Kim, “Solitonic behaviour in coupled multi atom–cavity systems,” *New Journal of Physics* **11**, 013059 (2009).
 [2] Neil V Corzo, Jérémy Raskop, Aveek Chandra, Alexandra S Sheremet, Baptiste Gouraud, and Julien Laurat, “Waveguide-coupled single collective excitation of atomic arrays,” *Nature* **566**, 359–362 (2019).
 [3] PJ Bardroff, I Bialynicki-Birula, Daniel S Krähler, G Kurizki,

- Erwin Mayr, Peter Stifter, and Wolfgang P Schleich, “Dynamical localization: Classical vs quantum oscillations in momentum spread of cold atoms,” *Physical review letters* **74**, 3959 (1995).
 [4] Wolfgang Niedenzu, Stefan Schütz, Hessam Habibian, Giovanna Morigi, and Helmut Ritsch, “Seeding patterns for self-organization of photons and atoms,” *Phys. Rev. A* **88**, 033830 (2013).

- [5] D. P. Craig and T. Thirunamachandran, *Molecular quantum electrodynamics: An introduction to radiation molecule interaction* (Dover Publications, 1998).
- [6] Ephraim Shahmoon, Pjotr Grišins, Hans Peter Stimming, Igor Mazets, and Gershon Kurizki, “Highly nonlocal optical nonlinearities in atoms trapped near a waveguide,” *Optica* **3**, 725–733 (2016).
- [7] Ephraim Shahmoon, Gershon Kurizki, Michael Fleischhauer, and David Petrosyan, “Strongly interacting photons in hollow-core waveguides,” *Physical Review A* **83**, 033806 (2011).
- [8] Inbal Friedler, David Petrosyan, Michael Fleischhauer, and Gershon Kurizki, “Long-range interactions and entanglement of slow single-photon pulses,” *Phys. Rev. A* **72**, 043803 (2005).
- [9] G. Kurizki, A. G. Kofman, and V. Yudson, “Resonant photon exchange by atom pairs in high- q cavities,” *Phys. Rev. A* **53**, R35–R38 (1996).
- [10] Philip W Anderson, “Absence of diffusion in certain random lattices,” *Physical review* **109**, 1492 (1958).
- [11] Mordechai Segev, Yaron Silberberg, and Demetrios N Christodoulides, “Anderson localization of light,” *Nature Photonics* **7**, 197–204 (2013).
- [12] Tobias Brandes and Stefan Kettemann, *Anderson localization and its ramifications: Disorder, phase coherence, and electron correlations*, Vol. 630 (Springer Science & Business Media, 2003).
- [13] Elihu Abrahams, *50 years of Anderson Localization*, Vol. 24 (world scientific, 2010).
- [14] Yosuke Nagaoka and Hidetoshi Fukuyama, *Anderson Localization: Proceedings of the Fourth Taniguchi International Symposium, Sanda-shi, Japan, November 3–8, 1981*, Vol. 39 (Springer Science & Business Media, 2012).
- [15] Andrej Anatol’evič Gogolin, “Electron localization and hopping conductivity in one-dimensional disordered systems,” *Physics Reports* **86**, 1–53 (1982).
- [16] Dmitry A Abanin, Ehud Altman, Immanuel Bloch, and Maksym Serbyn, “Colloquium: Many-body localization, thermalization, and entanglement,” *Reviews of Modern Physics* **91**, 021001 (2019).
- [17] Ronen Vosk, David A Huse, and Ehud Altman, “Theory of the many-body localization transition in one-dimensional systems,” *Physical Review X* **5**, 031032 (2015).
- [18] Carl W Helstrom, “Quantum detection and estimation theory,” *Journal of Statistical Physics* **1**, 231–252 (1969).
- [19] Matteo GA Paris, “Quantum estimation for quantum technology,” *International Journal of Quantum Information* **7**, 125–137 (2009).
- [20] Victor Mukherjee, Analia Zwick, Arnab Ghosh, Xi Chen, and Gershon Kurizki, “Enhanced precision bound of low-temperature quantum thermometry via dynamical control,” *Communications Physics* **2**, 162 (2019).
- [21] Nikolaos E. Palaodimopoulos, Maximilian Kiefer-Emmanouilidis, Gershon Kurizki, and David Petrosyan, “Excitation transfer in disordered spin chains with long-range exchange interactions,” *SciPost Phys. Core* **6**, 017 (2023).
- [22] Nicolò Defenu, Tobias Donner, Tommaso Macrì, Guido Pagano, Stefano Ruffo, and Andrea Trombettoni, “Long-range interacting quantum systems,” *Reviews of Modern Physics* **95**, 035002 (2023).
- [23] Alexandra S Sheremet, Mihail I Petrov, Ivan V Iorsh, Alexander V Poshakinskiy, and Alexander N Poddubny, “Waveguide quantum electrodynamics: collective radiance and photon-photon correlations,” *Reviews of Modern Physics* **95**, 015002 (2023).
- [24] Zbigniew Ficek and Stuart Swain, *Quantum interference and coherence: theory and experiments*, Vol. 100 (Springer Science & Business Media, 2005).
- [25] R. H. Lehberg, “Radiation from an n -atom system. i. general formalism,” *Phys. Rev. A* **2**, 883–888 (1970).
- [26] Stephan Ritter, Christian Nölleke, Carolin Hahn, Andreas Reiserer, Andreas Neuzner, Manuel Uphoff, Martin Mücke, Eden Figueroa, Joerg Bochmann, and Gerhard Rempe, “An elementary quantum network of single atoms in optical cavities,” *Nature* **484**, 195–200 (2012).
- [27] Freeman J Dyson, “Statistical theory of the energy levels of complex systems. i,” *Journal of Mathematical Physics* **3**, 140–156 (1962).
- [28] Gérard Ben Arous and Paul Bourgade, “Extreme gaps between eigenvalues of random matrices,” *The Annals of Probability* **41**, 2648 – 2681 (2013).
- [29] Géza Tóth and Iagoba Apellaniz, “Quantum metrology from a quantum information science perspective,” *Journal of Physics A: Mathematical and Theoretical* **47**, 424006 (2014).
- [30] Matteo G. A. Paris, “Quantum estimation for quantum technology,” *arXiv e-prints*, arXiv:0804.2981 (2008), arXiv:0804.2981 [quant-ph].
- [31] Nilakantha Meher, Eilon Poem, Tomáš Opatrný, Ofer Firstenberg, and Gershon Kurizki, “Supersensitive phase estimation by thermal light in a Kerr-nonlinear interferometric setup,” *Phys. Rev. A* **110**, 013715 (2024).
- [32] Chi Zhang and MR Tarbutt, “Quantum computation in a hybrid array of molecules and rydberg atoms,” *PRX Quantum* **3**, 030340 (2022).
- [33] F Kimiaee Asadi, SC Wein, and C Simon, “Protocols for long-distance quantum communication with single 167er ions,” *Quantum Science and Technology* **5**, 045015 (2020).
- [34] Mark Saffman, “Quantum computing with atomic qubits and rydberg interactions: progress and challenges,” *Journal of Physics B: Atomic, Molecular and Optical Physics* **49**, 202001 (2016).
- [35] Daniel Tiarks, Steffen Schmidt-Eberle, Thomas Stolz, Gerhard Rempe, and Stephan Dürr, “A photon–photon quantum gate based on rydberg interactions,” *Nature Physics* **15**, 124–126 (2019).
- [36] S-L Su, Li-Na Sun, B-J Liu, L-L Yan, M-H Yung, Weibin Li, and M Feng, “Rabi-and blockade-error-resilient all-geometric rydberg quantum gates,” *Physical Review Applied* **19**, 044007 (2023).
- [37] P. W. Anderson, “Absence of diffusion in certain random lattices,” *Phys. Rev.* **109**, 1492–1505 (1958).
- [38] D. L. Shepelyansky, “Coherent propagation of two interacting particles in a random potential,” *Phys. Rev. Lett.* **73**, 2607–2610 (1994).
- [39] Victor Mukherjee, Analia Zwick, Arnab Ghosh, Xi Chen, and Gershon Kurizki, “Enhanced precision bound of low-temperature quantum thermometry via dynamical control,” *Communications Physics* **2**, 162 (2019).
- [40] Piers Coleman and Andrew J Schofield, “Quantum criticality,” *Nature* **433**, 226–229 (2005).
- [41] Luca Pezzè, Marco Gabbriellini, Luca Lepori, and Augusto Smerzi, “Multipartite entanglement in topological quantum phases,” *Phys. Rev. Lett.* **119**, 250401 (2017).
- [42] Biao-Liang Ye, Li-Yuan Xue, Yu-Liang Fang, Sheng Liu, Qi-Cheng Wu, Yan-Hui Zhou, and Chui-Ping Yang, “Quantum coherence and quantum fisher information in the xxz system,” *Physica E: Low-dimensional Systems and Nanostructures* **115**, 113690 (2020).
- [43] Analia Zwick, Gonzalo A Álvarez, and Gershon Kurizki, “Maximizing information on the environment by dynamically

- controlled qubit probes,” *Physical Review Applied* **5**, 014007 (2016).
- [44] Nilakantha Meher, Tomáš Opatrný, and Gershon Kurizki, “Thermodynamic sensing of quantum nonlinear noise correlations,” *Quantum Science and Technology* **9**, 045029 (2024).
- [45] Bruno Ronchi, Analia Zwick, and Gonzalo A. Álvarez, “Maximizing information obtainable by quantum sensors through the quantum zeno effect,” *Phys. Rev. Appl.* **22**, 034058 (2024).
- [46] Note: $\int t^n e^{at} dt = e^{at} \sum_{p=0}^n t^p (-1)^{n-p} \frac{n!}{p! a^{n-p+1}}$ for $n > 0, a \neq 0$.
- [47] Gershon Kurizki and Abraham G. Kofman, “Bath-induced self-energy: Cooperative lamb-shift and dipole–dipole interactions,” in *Thermodynamics and Control of Open Quantum Systems* (Cambridge University Press, 2022) p. 91–118.
- [48] Gershon Kurizki, “Two-atom resonant radiative coupling in photonic band structures,” *Phys. Rev. A* **42**, 2915–2924 (1990).
- [49] Marlan O Scully, “Correlated spontaneous emission on the volga,” *Laser Physics* **17**, 635–646 (2007).
- [50] Anatoly A Svidzinsky, Jun-Tao Chang, and Marlan O Scully, “Dynamical evolution of correlated spontaneous emission of a single photon format from a uniformly excited cloud of n atoms,” *Physical review letters* **100**, 160504 (2008).

SUPPLEMENTARY INFORMATION

Two-atom case

Let us first consider the simplest scenario of only two TLAs. The Hamiltonian of the combined atom-cavity system is then given by

$$H = \omega_1|e_1\rangle\langle e_1| + \omega_2|e_2\rangle\langle e_2| + M(|e_1g_2\rangle\langle g_1e_2| + H.c.) + \omega a_0^\dagger a_0 + \sum_{\lambda} (\kappa_{1\lambda} a_0 |e_1\rangle\langle g_1| + \kappa_{2\lambda} a_0 |e_2\rangle\langle g_2| + H.c.). \quad (\text{S.1})$$

The Hamiltonian of the system leads to a general third-order polynomial equation for the evaluation of the eigenvalues, which of the form:

$$\lambda^3 - A\lambda^2 + B\lambda - C = 0, \quad (\text{S.2})$$

$A = (\omega + \omega_1 + \omega_2)$, $B = (\omega_1 + \omega_2)\omega + \omega_1\omega_2 - M^2 - \kappa_A^2$, $C = \frac{(\omega_1 + \omega_2)}{2}\omega + \kappa_A^2 \frac{(\omega_1 + \omega_2)}{2} + 2M\kappa_A\kappa_B - \kappa_B^2 - M\omega$. Here ω_1, ω_2 is the frequency of atom 1 and atom 2 respectively, and ω is the cavity frequency. To solve the general equation a variable change is executed, where we replace $\lambda = \Lambda + A/3$ and Eq. (S.2) reduces to

$$\Lambda^3 + p\Lambda + q = 0, \quad (\text{S.3})$$

where $p = (3B - A^2)/3$, and $q = (-2A^3 + 9AB - 27C)/27$. The roots are

$$\begin{aligned} \Lambda_1 &= \frac{1}{6^{2/3}(-9q + \sqrt{12p^3 + 81q^2})^{1/3}} \\ &\quad \times \left[-2\sqrt[3]{3}p + \sqrt[3]{2} \left(-9q + \sqrt{12p^3 + 81q^2} \right)^{1/3} \right], \\ \Lambda_2 &= \frac{1}{6^{2/3}(-9q + \sqrt{12p^3 + 81q^2})^{1/3}} \\ &\quad \times \left[\sqrt[3]{-1} \left(2\sqrt[3]{3}p + \sqrt[3]{-2}(-9q + \sqrt{12p^3 + 81q^2})^{1/3} \right) \right], \\ \Lambda_3 &= \frac{1}{6^{2/3}(-9q + \sqrt{12p^3 + 81q^2})^{1/3}} \\ &\quad \times \left[\sqrt[3]{-1} \left(2\sqrt[3]{-3}p + \sqrt[3]{2}(-9q + \sqrt{12p^3 + 81q^2})^{1/3} \right) \right] \end{aligned} \quad (\text{S.4})$$

For the specific values of the parameters as shown in Fig. 1c, we get a crossing, i.e., a degeneracy in the eigenvalues from Eq. (S.4). For the far zone case ($\kappa_a \neq \kappa_b$) there is no crossing in the eigenvalues.

In Laplace domain: The solution of the combined field-atom wave function $|\psi(t)\rangle$ in the Laplace domain can be written as in Eq. (3).

$$|\psi(t)\rangle = \sum_{j=1}^2 \alpha_j(t)|r_j\rangle + \beta(t)|1\rangle. \quad (\text{S.5})$$

Using Schrodinger's equation for time evolution we can rewrite the time-dependent coefficients α_j and β in the following form

$$\begin{aligned} \dot{\alpha}_j &= -i\omega_0\alpha_j - i\kappa_j\beta - i \sum_j M_{jj'}\alpha_{j'}, \\ \dot{\beta} &= -i\beta\omega - i \sum_j \alpha_j\kappa_j^*. \quad j = 1, 2 \end{aligned} \quad (\text{S.6})$$

Further, in the Laplace domain, the above set of coupled differential equations transforms into a set of coupled algebraic equations of the form,

$$\begin{aligned}
s\hat{\beta}(s) &= -i\omega\hat{\beta}(s) - i \sum_j \kappa_j^* \hat{\alpha}_j(s) + \beta(0), \quad j = 1, 2 \\
s\hat{\alpha}_j(s) &= -i\omega_0\hat{\alpha}_j(s) - i\kappa_j\hat{\beta}(s) - i \sum_{j'} M_{jj'} \hat{\alpha}_{j'}(s) + \alpha_j(0).
\end{aligned} \tag{S.7}$$

The solution to $\hat{\alpha}(s)$ in the two-atom case is

$$\begin{aligned}
\hat{\alpha}_1(s) &= |\mathcal{A}(s)|^{-1} \left(s + i\omega_2 + \frac{|\kappa_2|^2}{s + i\omega} \right), \\
\hat{\alpha}_2(s) &= -|\mathcal{A}(s)|^{-1}, \\
|\mathcal{A}(s)| &= M^2 - \frac{iM(\kappa_1^* \kappa_2 + \kappa_2^* \kappa_1)}{s + i\omega} + (s + i\omega_1)(s + i\omega_2) \\
&\quad + \frac{|\kappa_2|^2(s + i\omega_1)}{s + i\omega} + \frac{|\kappa_1|^2(s + i\omega_2)}{s + i\omega}.
\end{aligned} \tag{S.8}$$

Setting $s = -i\lambda$ in $|\mathcal{A}(s)| = 0$, gives the poles as a function of M . In the above expression, the polynomial has both linear and oscillatory terms for simple poles, whereas for at least one pole of order two in $|\mathcal{A}(s)|$ the polynomial is cubic rather than linear, apart from the oscillatory terms. For a particular value of M , say M_{cr} the point where the crossing of the eigenvalue occurs, i.e., the degeneracy of the eigenvalue occurs.

Photon-dressed multiatom network resonance via inverse Laplace transform

The solution of $\hat{\alpha}(s)$ for N atom system is

$$\hat{\alpha}(s) = \frac{\text{adj}(A(s))\alpha(0)}{|A(s)|} \tag{S.9}$$

The above fraction is a ratio of two polynomials. The fraction is a proper fraction (the degree of the denominator polynomial exceeds that of the numerator) because the numerator and the denominator polynomials have maximum degrees s^{2n-2} and s^{2n} respectively. If λ_m is the m th pole of order k_m of the denominator polynomial and it has total l distinct poles, the fraction can be expanded in the following partial fraction form,

$$\hat{\alpha}(s) = \frac{\text{adj}(A(s))\alpha(0)}{\prod_{m=1}^l (s - \lambda_m)^{k_m}} = \sum_{m=1}^l \sum_{j=1}^{k_m} \frac{\mathbf{r}_{m,j}}{(s - \lambda_m)^j}, \tag{S.10}$$

where, the k_q residues for q th pole are computed using the following formula

$$\mathbf{r}_{q,j} = \frac{1}{(k_q - j)!} \left. \frac{d^{k_q-j}}{ds^{k_q-j}} \left(\frac{\text{adj}(A(s))\alpha(0)}{\prod_{m=1, m \neq q}^l (s - \lambda_m)^{k_m}} \right) \right|_{s=\lambda_q}, \quad j = 1, \dots, k_q. \tag{S.11}$$

The inverse Laplace transform of the above expression yields,

$$\alpha(t) = \sum_{m=1}^l \sum_{j=1}^{k_m} \mathbf{r}_{m,j} \mathcal{L}^{-1} \left[\frac{1}{(s - \lambda_m)^j} \right] = \sum_{m=1}^l \sum_{j=1}^{k_m} \frac{\mathbf{r}_{m,j}}{(j-1)!} t^{j-1} e^{\lambda_m t} = \sum_{m=1}^l \sum_{j=1}^{k_m} \mathbf{A}_{m,j} t^{j-1} e^{\lambda_m t}. \tag{S.12}$$

Therefore, the transition probability of the first atom averaged over time T can be written as

$$\bar{P}_A = \frac{1}{T} \int_0^T |\alpha_1(t)|^2 dt = \sum_{m=1}^l \sum_{m'=1}^l \sum_{j=1}^{k_m} \sum_{j'=1}^{k_{m'}} \mathbf{A}_{m,j}^{1*} \cdot \mathbf{A}_{m',j'} \int_0^T dt t^{(j+j')-2} e^{t(\lambda_m^* + \lambda_{m'})}. \tag{S.13}$$

Solving the definite integral, we obtain

$$\bar{P}_A = \frac{1}{T} \int_0^T |\alpha_1(t)|^2 dt = \sum_{m=1}^l \sum_{m'=1}^l \sum_{j=1}^{k_m} \sum_{j'=1}^{k_{m'}} A^{1*}_{m',j'} A^1_{m,j} I_{m,m',j,j'}(T), \quad (\text{S.14a})$$

where [46]

$$\begin{aligned} I_{m,m',j,j'}(T) &= \sum_{p=0}^{(j+j')-2} \frac{(-1)^{(j+j')-p-2} (j+j'-2)!}{p!((\lambda_{m'}^* + \lambda_m))^{(j+j')-p-1}} e^{T(\lambda_{m'}^* + \lambda_m)} T^p \quad \text{for } j+j' > 2, \lambda_m + \lambda_{m'}^* \neq 0, \\ I_{m,m',j,j'}(T) &= \frac{e^{T(\lambda_{m'}^* + \lambda_m)} - 1}{(\lambda_{m'}^* + \lambda_m)} \quad \text{for } j+j' = 2, \lambda_m + \lambda_{m'}^* \neq 0, \\ I_{m,m',j,j'}(T) &= \frac{T^{j+j'-1}}{j+j'-1} \quad \text{for } \lambda_m + \lambda_{m'}^* = 0. \end{aligned} \quad (\text{S.14b})$$

This crossing in turn gives rise to divergence in the residue. Equation (14b) will then be given by

$$\begin{aligned} \bar{P}_A &= \frac{1}{T} \int_0^T |\alpha_1(t)|^2 dt = \sum_{m=1}^l \sum_{m'=1}^l \sum_{j=1}^{k_m} \sum_{j'=1}^{k_{m'}} A^{1*}_{m',j'} A^1_{m,j} \frac{T^{j+j'-1}}{j+j'-1} \\ &+ \sum_{m=1}^l \sum_{m'=1}^l \sum_{j=1}^{k_m} \sum_{j'=1}^{k_{m'}} \sum_{p=0}^{j+j'-2} A^{1*}_{m',j'} A^1_{m,j} \frac{(-1)^{(j+j')-p-2} (j+j'-2)!}{p!((\lambda_{m'}^* + \lambda_m))^{(j+j')-p-1}} T^p e^{T(\lambda_{m'}^* + \lambda_m)} \\ &+ \sum_{m,m'} A^{1*}_{m',j'} A^1_{m,j} \frac{e^{T(\lambda_{m'}^* + \lambda_m)}}{\lambda_m + \lambda_{m'}^*} + \text{constant}, \end{aligned} \quad (\text{S.15})$$

which can be rewritten as

$$\begin{aligned} \bar{P}_A &= \frac{1}{T} \int_0^T |\alpha_1(t)|^2 dt = \sum_{j=1}^{k_m} \sum_{j'=1}^{k_{m'}} X_{j,j'} T^{j+j'-1} \\ &+ \sum_{m=1}^l \sum_{m'=1}^l \sum_{j=1}^{k_m} \sum_{j'=1}^{k_{m'}} \sum_{p=0}^{j+j'-2} Y_{m,m',j,j',p} T^p e^{T(\lambda_{m'}^* + \lambda_m)} \\ &+ \sum_{m,m'} Z_{m,m'} e^{T(\lambda_{m'}^* + \lambda_m)} + \text{constant}. \end{aligned} \quad (\text{S.16})$$

Effect of Randomness

The effects of randomness in PIMATE are shown in Fig. S1. This randomness transforms the crossing points in the eigenvalue spectrum into pseudo-crossings. As a result, distinct peaks in the time-averaged excitation probability distribution are no longer observed.

Dissipative effects

In the long-range NNN regime, if we consider the collective dissipation to be large, $\gamma \sim \gamma_{ij} \sim M_{ij}$, then the crossing points disappear due to the decay, but pseudo crossing points are still observed for $N = 8$ for the perfectly ordered chains (Fig. S2a). In the case of the randomized chains, even the pseudo-crossing points get washed out. Namely, randomness along with dissipation washout the effect of pseudo-crossing from the eigenvalue spectrum. Excitation delocalization due to the presence of large dissipation in the long-range NNN interaction regime, without the randomness is shown in Fig. S2b. For polarization parallel or perpendicular to the inter-atom axis the matrix of radiative dissipative rates is [25]

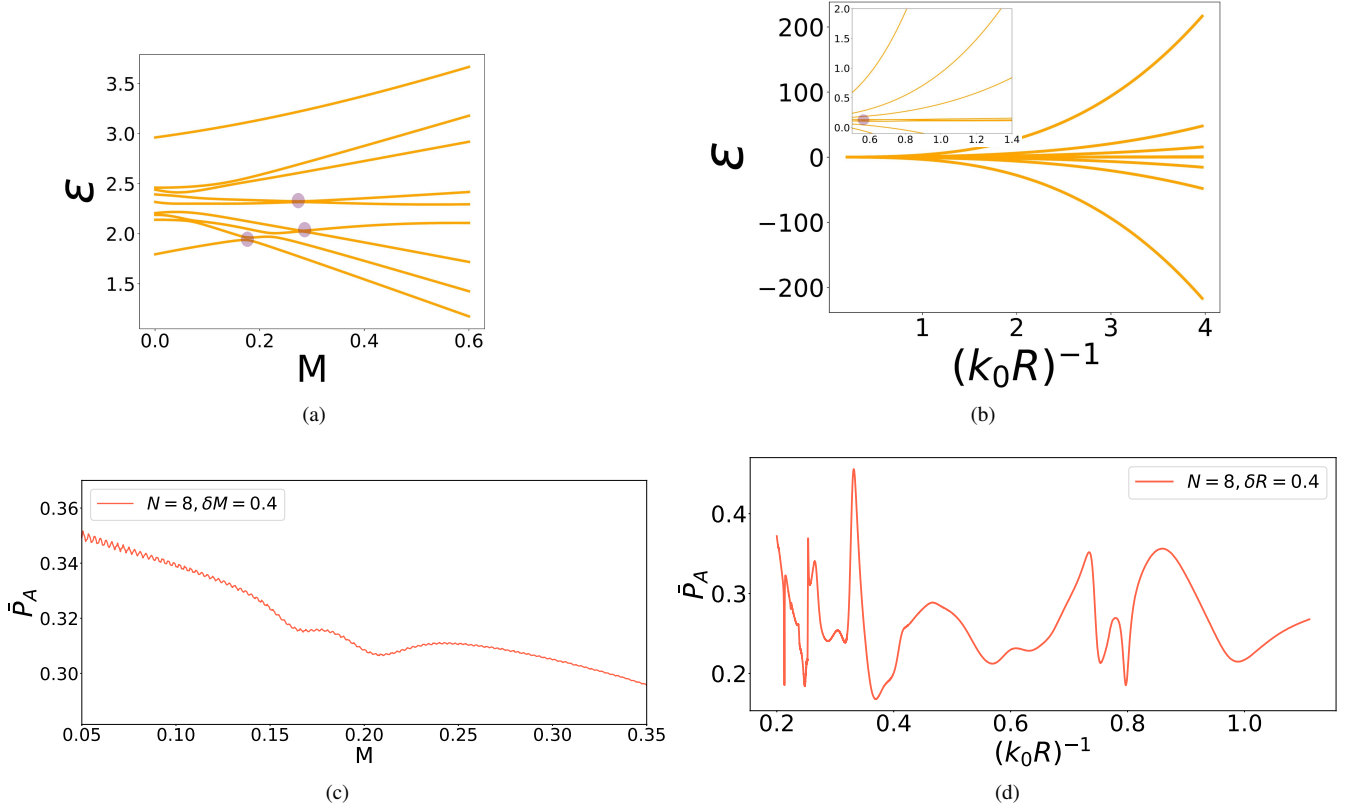


FIG. S1: (a), (b) Eigenvalue dependence on M or k_0R for the same parameters as in Fig. 1, 2, but in the presence of off-diagonal randomness with standard deviation = 0.4. The crossing and the pseudo-crossing are marked by circles. (c) Resonances of the time-averaged excitation probability as a function of M (dipole-dipole interaction strength) with negligible dissipation for the NN interaction indicating that trapping vanishes with the high randomness in the system, (d) Same, for the long-range NNN interaction with randomness as a function of k_0R that indicates partial trapping. The Hamiltonian parameters are $\omega - \omega_0 = 0.2\gamma$, $T = 10000$, $\kappa_j = 0.2\gamma$.

$$\begin{aligned}\gamma_{ij} &= \gamma f_{\Sigma}(k_0R_{ij}), \\ \gamma_{ij} &= \gamma f_{\Pi}(k_0R_{ij}),\end{aligned}\tag{S.17a}$$

where

$$\begin{aligned}f_{\Sigma}(k_0R_{ij}) &= 3 \left[\frac{\sin(k_0R_{ij})}{(k_0R_{ij})^3} - \frac{\cos(k_0R_{ij})}{(k_0R_{ij})^2} \right], \\ f_{\Pi}(k_0R_{ij}) &= -\frac{3}{2} \left[\frac{\sin(k_0R_{ij})}{(k_0R_{ij})^3} - \frac{\cos(k_0R_{ij})}{(k_0R_{ij})^2} - \frac{\sin(k_0R_{ij})}{(k_0R_{ij})} \right].\end{aligned}\tag{S.17b}$$

In the near zone, $k_0R_{ij} \ll 1$, the radiative rates $\gamma_{ij}/\gamma = f_{\Pi(\Sigma)}(k_0R_{ij}) \rightarrow 1$ are *negligible* compared to the RDDI $\text{Re}(M_{ij}) \sim \cos(k_0R_{ij})/(k_0R_{ij})^3$. In the far zone, $k_0R_{ij} \gtrsim 1$, the ratio $\gamma_{ij}/M_{ij} \rightarrow 1$ and we may estimate the dissipative effects by replacing $\gamma_{ij} \rightarrow \gamma$. However, γ and γ_{ij} can be drastically *suppressed* in cavities or waveguides by placing the resonant transition frequency $\omega_0 = k_0c$ inside a *photonic band gap* where M_{ij} remains essentially undiminished [6, 7, 47, 48].

Thus, we can address one of two possible regimes: either negligible dissipation compared to RDDI, $\gamma_{ij} \ll M_{ij}$, or dissipation that is comparable to RDDI, $\gamma \gtrsim \gamma_{ij} \sim M_{ij}$. The effects of dissipation in PIMATE are shown in Fig. S2. In the presence of dissipation transforms the crossing points in the eigenvalue spectrum into pseudo-crossings. As a result, distinct peaks in the time-averaged excitation probability distribution are no longer observed. With the randomness being introduced along with the presence of dissipation we don't have even pseudo-crossing thus a loss of QFI divergence.

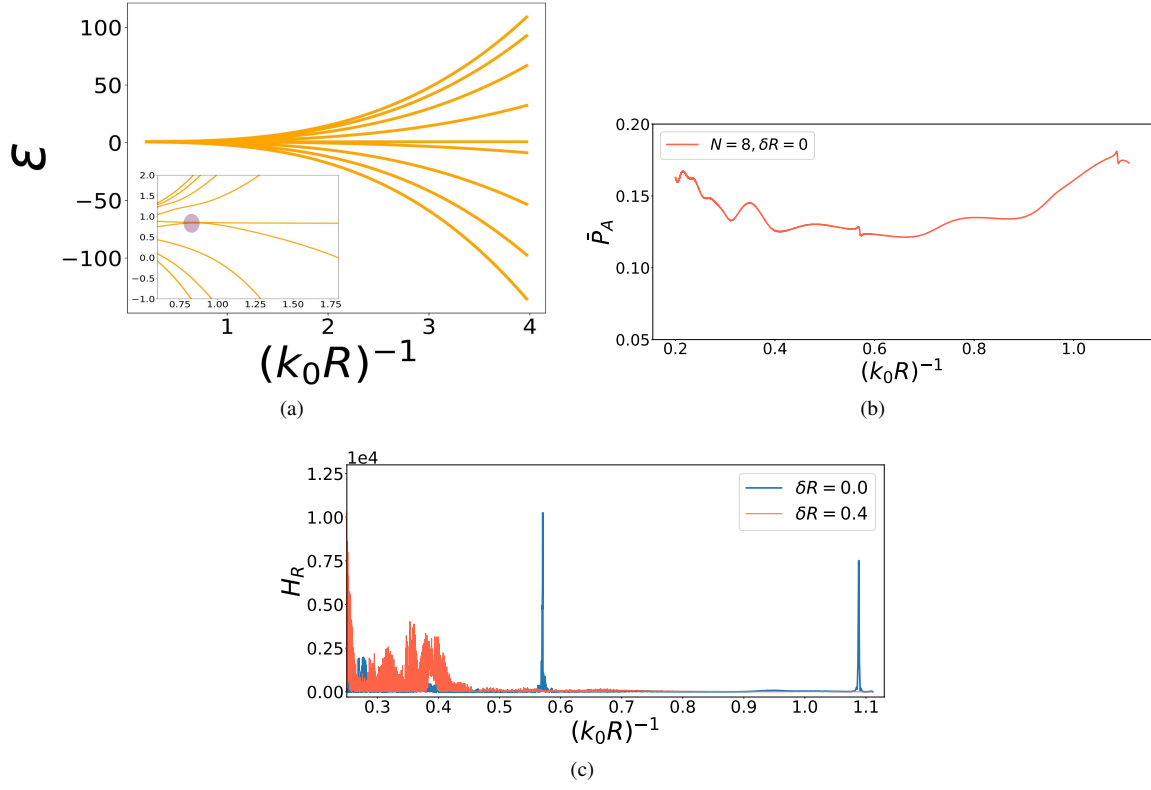


FIG. S2: (a) Change of crossing points to pseudo-crossings as a function of separation k_0R for large dissipation (collective dissipation rate $\gamma_{ij}/M \rightarrow 1$). The pseudo-crossing points of eigenvalues on all plots are marked by circles. (b) Resonances of the time-averaged excitation probability as a function of k_0R for large dissipation (collective dissipation rate $\gamma_{ij}/M \rightarrow 1$). The dips exhibit suppressed (*anti-*) trapping. (c) Variation of the quantum Fisher information for large dissipation ($\gamma_{ij}/M \rightarrow 1$) in the presence of off-diagonal randomness (red solid line) and without randomness (blue solid line).

Time-domain evolution in the computational and Dicke bases

The atom-field system with atom 1 initially excited, the state vector for the atom-field system at time t [49, 50] has the following state in the Dicke basis

$$|\psi(t)\rangle = \left[\eta_+(t)|+\rangle + \sum_{j=1}^{N-1} \zeta_j |j\rangle \right] |0\rangle + \nu(t) |g, \dots, g\rangle |1\rangle. \quad (\text{S.18})$$

Here first term with amplitude $\eta_+(t)$ corresponds to the state which is prepared by uniformly absorbing a single photon with wavevector k_0 , $|+_{k_0}\rangle = \frac{1}{\sqrt{N}} \sum_k e^{ik_0 X_k} |e, \dots, r_k, \dots, e\rangle$. The subsequent terms with amplitude ζ_j corresponds to Dicke states $|j\rangle$, where $|j=1\rangle = \frac{1}{\sqrt{2}} [e^{ik_0 X_1} |r_1\rangle - e^{ik_0 X_2} |r_1\rangle]$ and the state $|j=N-1\rangle = \frac{1}{\sqrt{N-1}} [e^{ik_0 X_1} |r_1\rangle + e^{ik_0 X_2} |r_2\rangle + e^{ik_0 X_3} |r_3\rangle + \dots + e^{ik_0 X_{N-1}} |r_{N-1}\rangle - (N-1)e^{ik_0 X_N} |r_N\rangle]$. The time-averaged excitation probabilities for $N=8$ show equivalent results for the time-dependent trapping in both the computational and the Dicke bases consistent with Fig. 3.

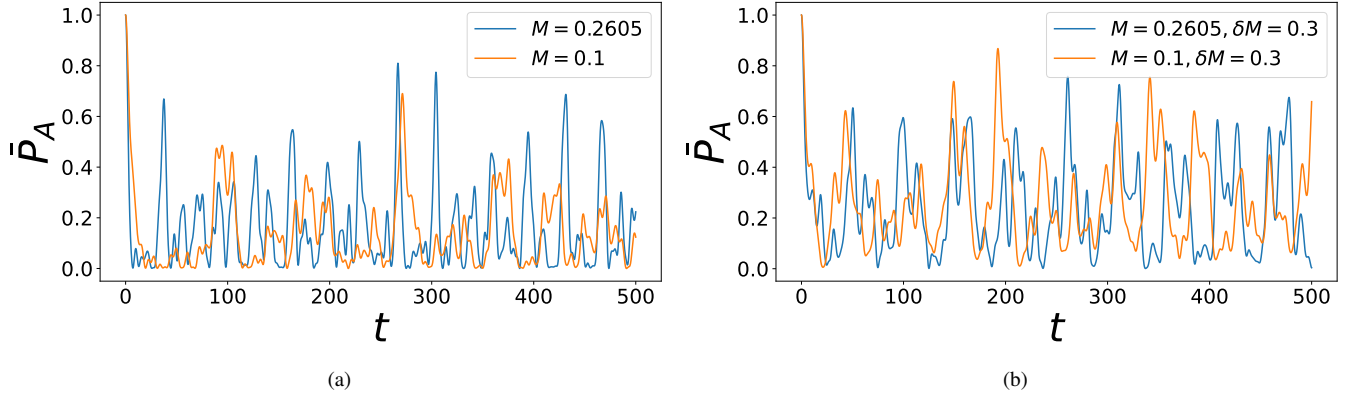


FIG. S3: (a) Time dependence of excitation probability for the first atom out of $N = 4$ at the crossing point (resonance point) $M = M_{cr}$ (blue solid line) and non-resonance point (orange solid line). (b) Same in the presence of randomness at the crossing point (blue solid line) and non-resonance point (orange solid line). The parameter are as in Fig. 3.

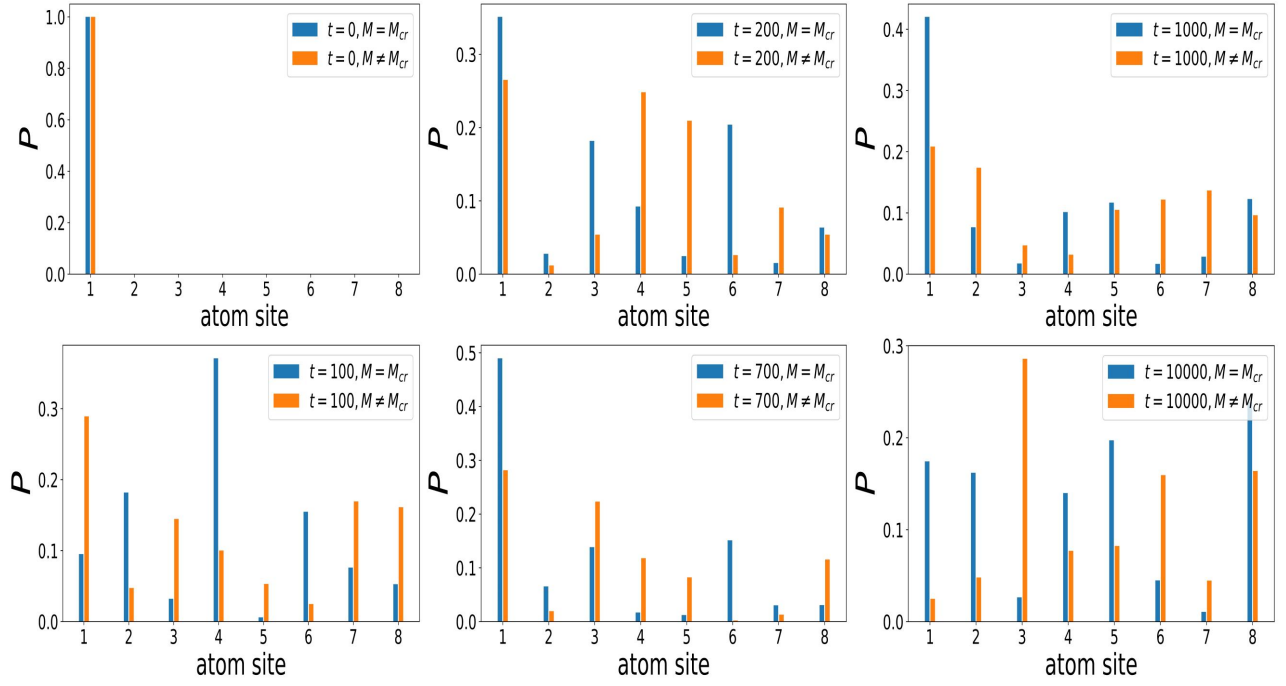


FIG. S4: Time dependence of excitation probability with the atom sites at the crossing point $M = M_{cr}$ in blue. Same at a non-resonance point in orange. Fig. 3.

Fisher information under randomness

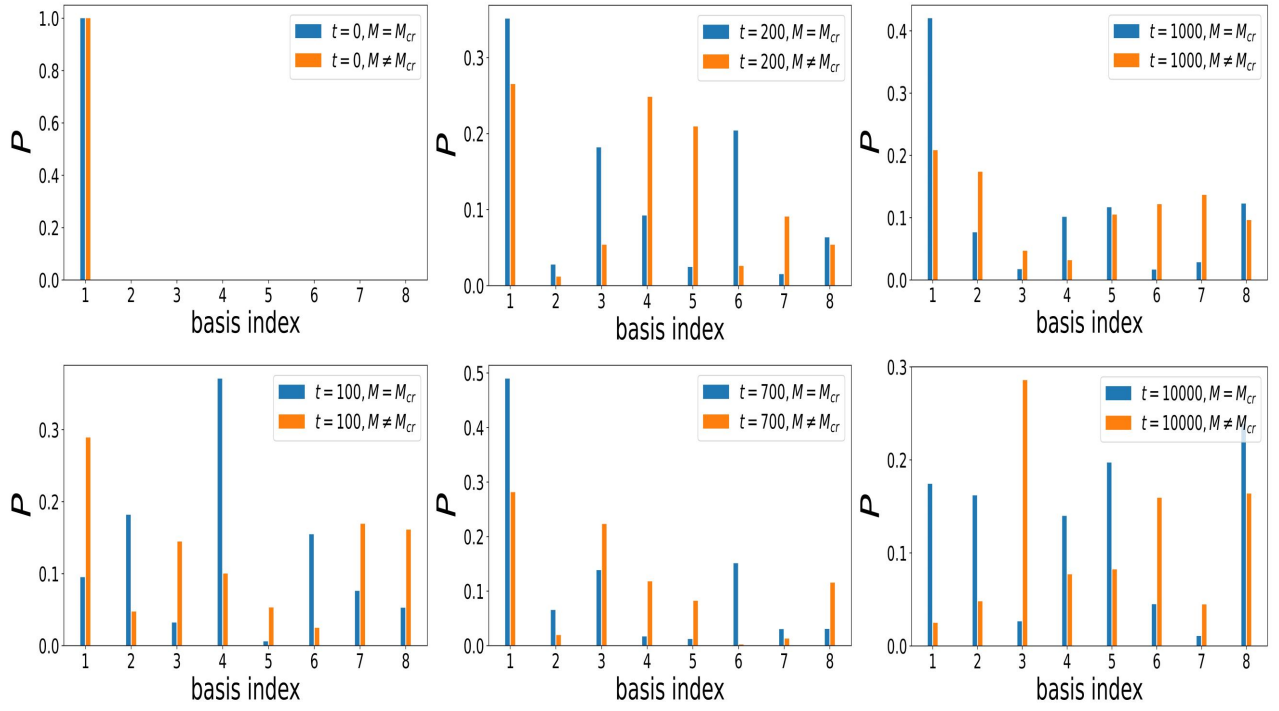


FIG. S5: Time dependence of excitation probability in the transformed Dicke basis (described as basis indices) at the crossing/resonance point $M = M_{cr}$ (in blue) and the non-resonant point (in orange).

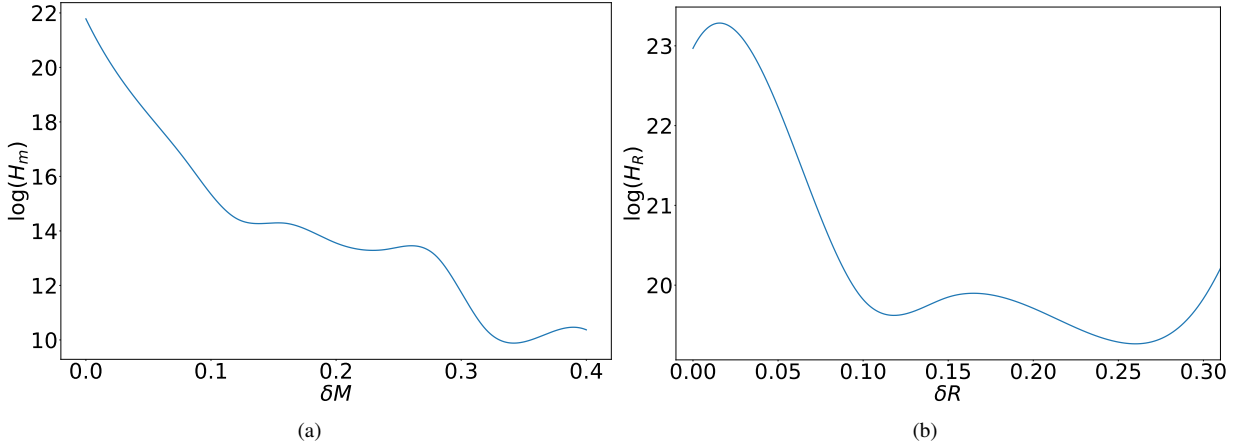


FIG. S6: (a) The variation of the logarithmic quantum Fisher information for $N = 8$ as a function of randomness in M (dipole-dipole interaction strength) for the nearest neighbor interaction. (b) Same for the long-range interaction.

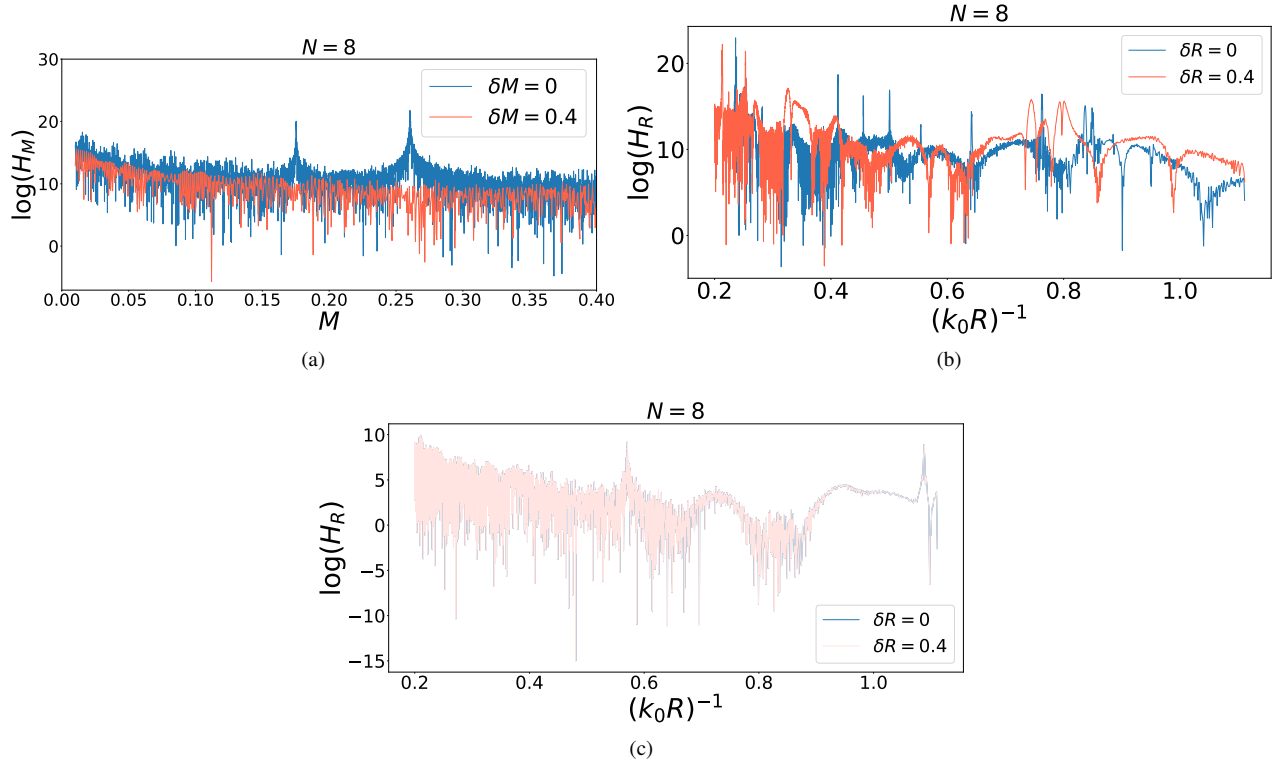


FIG. S7: (a) The variation of the logarithm of the quantum Fisher information in the NN regime without dissipation for $N = 8$ as a function of M (dipole-dipole interaction strength) in the presence of randomness (red solid line) and without randomness (black solid line). (b) Same for the long-range NNN interaction as a function of $1/(k_0 R)$ (for negligible dissipation $\gamma_{ij}/M \rightarrow 0$) in the presence of randomness (red solid line) and without randomness (black solid line). (c) Same for comparable dissipation ($\gamma_{ij}/M \rightarrow 1$) in the presence of randomness (red solid line) and without randomness (black solid line). The Hamiltonian parameters $\omega - \omega_0 = 0.2\gamma$, $\kappa_j = 0.2\gamma$, $T = 10000$.